

Preliminary study on the potential use of *Averrhoa bilimbi* L. as a supercapacitor electrode material

Lailatul Rahmi, Awitdrus*

Department of Physics, Universitas Riau, Pekanbaru 28293, Indonesia

*Corresponding author: awitdrus@lecturer.unri.ac.id

ABSTRACT

The global energy crisis and environmental damage caused by the use of fossil fuels have driven the development of environmentally friendly energy storage technologies, one of which is the supercapacitor. This study aims to explore the potential of *Averrhoa bilimbi* L. (belimbing wuluh) as a source of activated carbon for supercapacitor applications. Activated carbon from belimbing wuluh pulp was synthesized through a carbonization process at 800°C. Morphological characterization using SEM showed a porous surface that had not yet developed optimally, while EDX analysis identified carbon, oxygen, and magnesium as the dominant elements. Electrochemical characterization was carried out using CV and GCD methods with variations in H₂SO₄ electrolyte concentration (1, 2, and 3 M). The electrode tested with 1 M showed the best performance, with a specific capacitance of 45.98 F/g (CV) and 96.81 F/g (GCD). These results indicate that belimbing wuluh has potential as a sustainable natural material for the development of environmentally friendly supercapacitors.

Keywords: Belimbing wuluh; non-activated carbon; supercapacitor; sulfuric acid

Received 12-05-2025 | Revised 26-05-2025 | Accepted 03-06-2025 | Published 31-07-2025

INTRODUCTION

The global energy crisis and environmental degradation caused by the use of fossil fuels have become critical issues driving the development of more environmentally friendly energy storage technologies, such as supercapacitors [1]. In addition, the growth of the world population, which has reached 8 billion people, further exacerbates energy problems, as each individual consumes energy every second in various forms [2]. Supercapacitors typically store energy through physical charge separation, unlike batteries that rely on chemical reactions for energy storage. The working principle of supercapacitors depends on the electric charge carried by ions [3]. The main components of a supercapacitor include the electrolyte, current collector, electrode, and separator material [4].

The performance of supercapacitors heavily depends on the unique characteristics of the electrode materials used. Therefore, it is essential to investigate electrode materials in order to maximize the potential of

supercapacitors [5]. Various types of biomass have been extensively studied for supercapacitor development. A wide range of natural resources including agricultural waste such as rice husks [6] and wheat straw [7], plant parts such as cinnamon sticks [8] and bamboo [9], as well as fruits like Japanese citron [10] and orange peels [11] have been explored. In addition, unique materials such as strobili fibers [12] and stone pine [13] have also been tested for their potential [14].

Belimbing wuluh is tropical plant is widely available and is not a seasonal crop [15]. The fruit is oval-shaped, measuring approximately 4 – 6 cm in length, with a glossy skin that ranges in color from green to yellow. Annual fruit production can reach up to 1,500 fruits per plant. The productivity or yield characteristics can be observed from the number of fruits produced per plant [16]. Belimbing wuluh contains various chemical components, including phenols, flavonoids, pectin, saponins, tannins, glycosides, and is also rich in minerals [17].

This research is a preliminary study aimed at exploring the utilization of carbon derived from belimbing wuluh. without chemical activation as an electrode material for supercapacitors. The carbon was obtained through a Carbonization process under a nitrogen (N_2) atmosphere and subsequently used as the active material for the electrode. Sulfuric acid (H_2SO_4) solution was employed as the electrolyte, with varying concentrations of 1M, 2M, and 3M, to investigate the effect of electrolyte concentration on the specific capacitance of the resulting supercapacitor.

RESEARCH METHODS

Materials

This study used belimbing wuluh collected from the Universitas Riau area. Starch flour was used to adhere the sample to the electrode plate, and H_2SO_4 (sulfuric acid) solutions with concentrations of 1, 2, and 3 M were used as the electrolytes.

Method

The belimbing wuluh biomass was washed, pressed, and then sun-dried for 2 – 3 days until a constant mass was achieved. Once dried, the biomass underwent a pre-carbonization process at 200°C for 30 minutes, followed by grinding and blending to obtain a fine carbon powder. The powder was then sieved using a 53-micrometer mesh with the aid of a brush to achieve a uniform particle size. Next, the sample was subjected to stepwise heating in a furnace: from room temperature to 400°C at a rate of 5°C/min over 1 hour and 14 minutes, held for 1 hour; then increased to 600°C over 40 minutes, held for another hour; and finally raised to 800°C over 40 minutes and maintained for 2 hours. This entire process was carried out in a closed system under a nitrogen (N_2) atmosphere. After pyrolysis, the carbon was cooled to room temperature and neutralized by rinsing with distilled water for 3 – 4 days until a neutral pH (~7) was achieved. The sample was

then dried in an oven at 110°C for 24 hours. For electrode fabrication, 0.1 grams of carbon powder was mixed with a starch solution (2 grams of starch flour in 20 mL of distilled water), which was heated and stirred. The resulting carbon paste was applied onto a stainless steel current collector. Whatman paper was used as a separator to assemble the supercapacitor cell. The steps involved in preparing the sample into a supercapacitor electrode are illustrated in Figure 1 below.

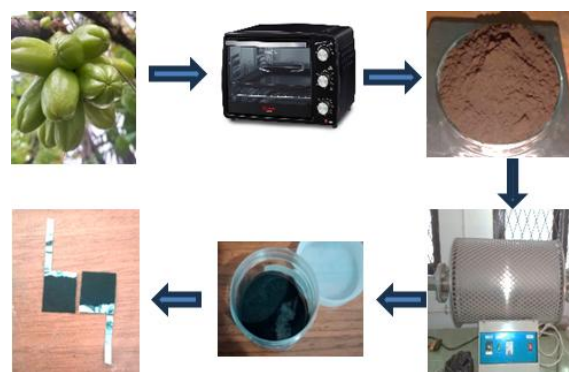


Figure 1. Sample fabrication process.

Characterization

Physical characterization using scanning electron microscopy (SEM) produces microscopic images of the carbon electrode. These images allow for the observation of pore shapes and sizes on both the surface and internal structure of the electrode. SEM data provides crucial information about the morphological characteristics of the electrode material derived from bilimbi fruit. Meanwhile, energy dispersive X-ray (EDX) analysis offers detailed information about the elemental composition of the activated carbon electrode produced from bilimbi fruit. This data can be further used to analyze the material's intrinsic properties.

Electrochemical Study

Electrochemical characterization was conducted using cyclic voltammetry (CV). From the CV tests, charging and discharging current data were obtained, which were then

used to calculate the specific capacitance value using Equation (1) as shown below [18]:

$$C_{sp} = \frac{(I_c - I_d)}{s \times m} \quad (1)$$

Characterization using galvanostatic charge-discharge (GCD) was performed to further evaluate the electrochemical performance of the electrode. The data obtained from the GCD test were subsequently used to calculate the specific capacitance value using Equation (2) as follows [19]:

$$C_{sp} = \frac{2 I \cdot \Delta t}{m \cdot \Delta V} \quad (2)$$

RESULTS AND DISCUSSION

Surface Morphology Analysis

Scanning Electron Microscopy (SEM) characterization was carried out to observe the surface morphology and pore size distribution of the bilimbi-derived carbon electrode. Figure 2 presents the SEM image of the carbon electrode at 1000x magnification. The SEM micrograph reveals that the carbon material possesses an irregular, stacked particle structure, forming a dense and interconnected surface. This type of morphology may contribute to good mechanical strength and structural stability, which are beneficial for maintaining the integrity of the electrode during supercapacitor operation.

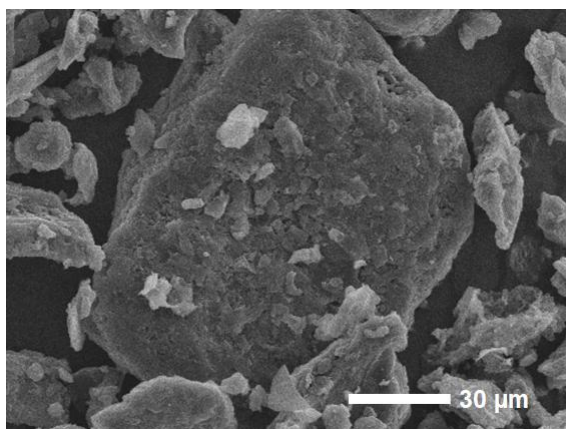


Figure 2. SEM characterization results.

The relatively smooth surface and minimal pore presence indicate that the carbonization process produced a compact material. However, the limited number of open pores may reduce the available active surface area for electrolyte ion interaction. This can affect electrochemical performance, particularly in terms of specific capacitance and charge transfer efficiency [20]. In other words, although the resulting structure is stable and well-integrated, further development of porosity is still necessary to optimize the energy storage characteristics of this material.

Elemental Composition Analysis

Based on the results of Energy Dispersive X-ray (EDX) analysis, the carbon material was found to be predominantly composed of carbon, with an atomic percentage of 92.66%. This high carbon content indicates that the carbonization process successfully produced a carbon-rich structure, which is essential for supercapacitor electrode materials. In addition to carbon, oxygen was also detected at 7.14%, likely originating from residual oxygen-containing functional groups such as hydroxyl, carbonyl, or carboxyl on the material's surface. These groups play a crucial role in enhancing hydrophilicity and interactions with electrolyte ions, thereby supporting electrochemical performance [21]. Furthermore, a small amount of magnesium (0.20% atomic) was identified, which may be attributed to residual inorganic compounds from the synthesis process or the original raw material. The presence of these elements provides a comprehensive understanding of the material's chemical composition and its potential contribution to electrode performance.

Electrochemical Characterization

The CV test results in the form of curves can be seen in Figure 3. The shape of the curve, which approaches a rectangular profile, indicates that the charge storage mechanism in this carbon material occurs via electric double

layer capacitance (EDLC), characterized by a stable and reversible electrochemical response. The specific capacitance values of each sample were determined based on the cathodic (I_c) and anodic (I_d) current data obtained at a scan rate of 5 mV/s.

The I_c value represents the maximum current during the reduction process (charge storage), while the I_d value corresponds to the maximum current during the oxidation process (charge release). These two current values are used to calculate the area under the CV curve, which is then converted into the specific capacitance value [22].

The calculation results show that the electrolyte with a concentration of 1M yields

the highest specific capacitance of 45.98 F/g, followed by 2M at 41.10 F/g, and the lowest at 3M with 20.75 F/g at a scan rate 5 mV/s. This trend indicates that increasing the electrolyte concentration does not necessarily enhance the material's performance. At higher concentrations such as 3 M, the solution's viscosity increases, which hinders ion diffusion into the electrode pores [23]. Therefore, it can be concluded that the optimal electrolyte concentration of bilimbi fruit-based aqueous solution in this system is 1M, as it provides the most efficient charge transfer and the highest specific capacitance, in accordance with the observations from the previous CV curve analysis.

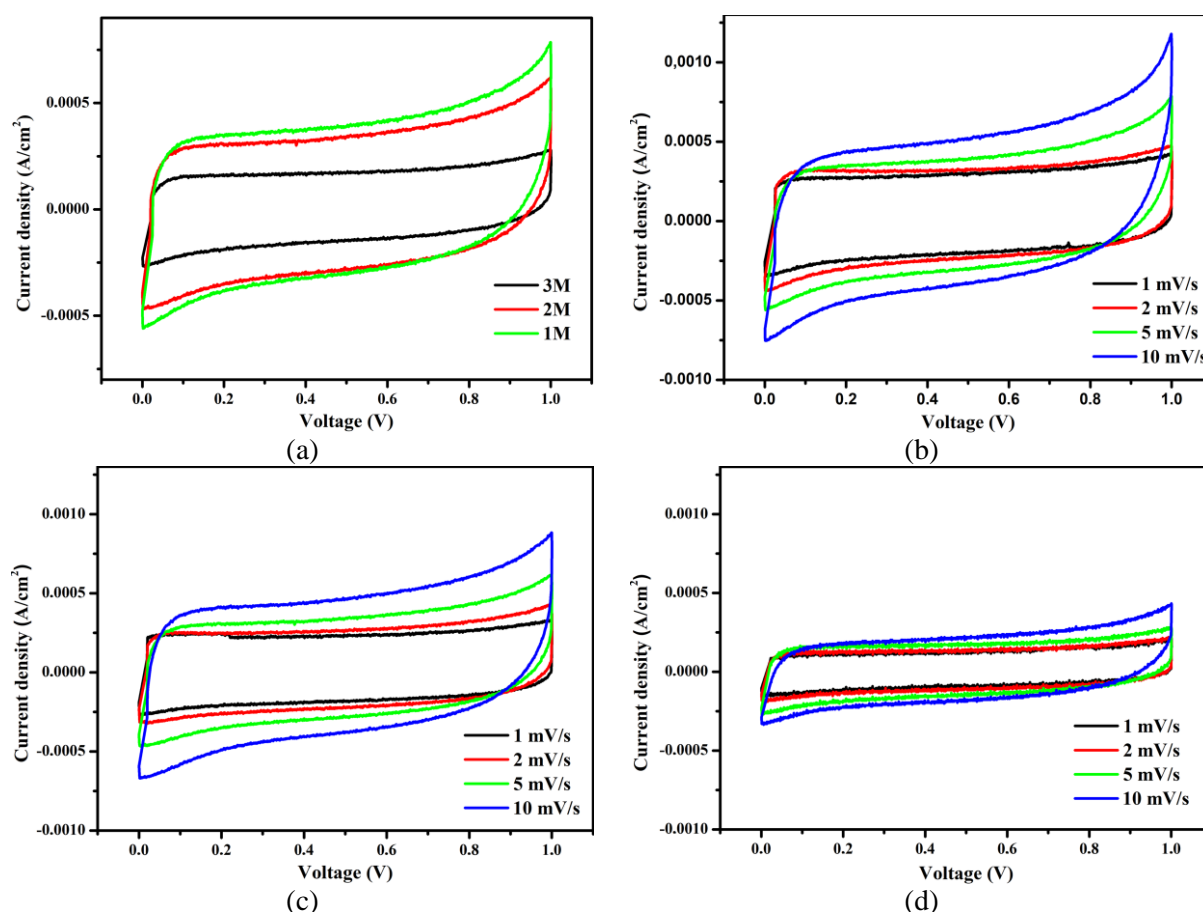


Figure 3. CV curves at different concentrations: (a) scan rate 5 mV/s for comparison (b) 1 M, (c) 2 M, (d) 3 M.

Figure 4 shows the GCD curves of the sample-based electrolyte concentrations, illustrating how the performance of the electrodes varies with different electrolyte strengths. The curves exhibit a nearly triangular

shape, indicating good capacitive behavior, and show that the charge–discharge process occurs in a highly reversible manner. This triangular shape reflects the ideal behavior of an electric double-layer capacitor, confirming that the

electrodes can store and release charge effectively without significant resistance or polarization. The data also suggest that the electrode structure is stable and efficient in different electrolyte environments.

Based on the GCD curve shown in Figure 4, it can be observed that the discharge time increases as the electrolyte concentration decreases. This indicates that the specific capacitance increases with decreasing electrolyte concentration, with values of 30.33

F/g for 3M, 38.48 F/g for 2M, and 56.61 F/g for 1M, respectively. The GCD curve demonstrates that the discharge profile for the 1M electrolytes exhibits the longest discharge time, indicating a higher charge storage capability compared to higher concentrations. This phenomenon may be attributed to reduced viscosity and enhanced ion diffusion at lower concentrations, allowing for more efficient charge transfer during the discharge process.

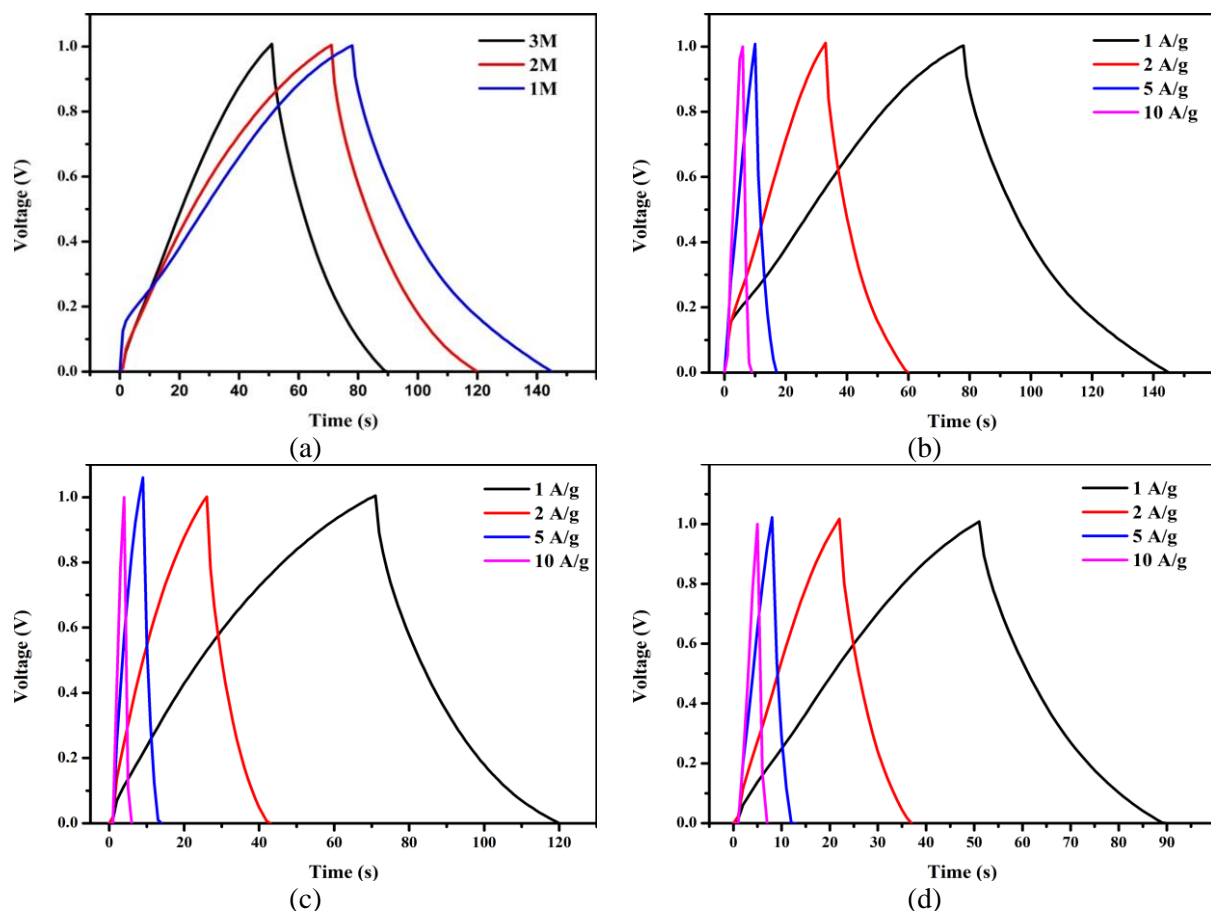


Figure 4. GCD curves at different concentrations: (a) rapat arus 1 A/g for comparison, (b) 1 M, (c) 2 M, (d) 3 M.

The specific capacitance obtained from the GCD method is generally lower compared to the values calculated using CV. This discrepancy is attributed to differences in testing duration, where CV typically involves a longer scan time, allowing the system greater opportunity to absorb and store charge more effectively. Consequently, although CV tends to yield higher capacitance values, the capacitance derived from GCD more accurately

represents the actual performance of the electrode under constant current operational conditions [24].

CONCLUSION

This study demonstrated that the type of separator material significantly influences the electrochemical performance of activated carbon electrodes derived from orange peel

biomass for supercapacitor applications. Among the three separators tested Whatman filter paper no. 40 (JR-800-W), eggshell membrane (JR-800-E), and orange fruit membrane (JR-800-O) the JR-800-W sample consistently exhibited the highest specific capacitance in both CV (191.82 F/g) and GCD (174.24 F/g) analyses. This superior performance is attributed to the uniform microporous structure and excellent electrolyte absorption of Whatman paper, which promotes faster ion diffusion and more efficient electric double-layer formation. The eggshell membrane separator (JR-800-E) showed moderate performance, with sufficient ionic mobility but slightly higher internal resistance. Meanwhile, the orange fruit membrane (JR-800-O) demonstrated the lowest performance due to its dense, non-uniform structure and limited electrolyte uptake, resulting in reduced ion transport and higher IR drop. These findings affirm that choosing a separator with high porosity, good wettability, and mechanical stability is critical to optimizing the energy storage efficiency and cycling stability of supercapacitor devices.

REFERENCES

1. Zhang, Q., & Wei, K. (2024). A comparative study of fractional-order models for supercapacitors in electric vehicles. *International Journal of Electrochemical Science*, **19**(1), 100441.
2. Phor, L., Kumar, A., & Chahal, S. (2024). Electrode materials for supercapacitors: A comprehensive review of advancements and performance. *Journal of Energy Storage*, **84**, 110698.
3. Wang, Q., Ma, Y., Liang, X., Zhang, D., & Miao, M. (2019). Flexible supercapacitors based on carbon nanotube-MnO₂ nanocomposite film electrode. *Chemical Engineering Journal*, **371**, 145–153.
4. Zhang, J., Gu, M., & Chen, X. (2023). Supercapacitors for renewable energy applications: A review. *Micro and Nano Engineering*, **21**, 100229.
5. Vazhayil, A., Thomas, J., Thomas, T., Hasan, I., & Thomas, N. (2024). Mn-substituted NiCo₂O₄/rGO composite electrode for supercapacitors and their electrochemical performance boost by redox additive in alkaline electrolyte. *Journal of Energy Storage*, **84**, 110789.
6. Arkhipova, E. A., Novotortsev, R. Y., Ivanov, A. S., Maslakov, K. I., & Savilov, S. V. (2022). Rice husk-derived activated carbon electrode in redox-active electrolyte—new approach for enhancing supercapacitor performance. *Journal of Energy Storage*, **55**, 105699.
7. Gou, G., Huang, F., Jiang, M., Li, J., & Zhou, Z. (2020). Hierarchical porous carbon electrode materials for supercapacitor developed from wheat straw cellulosic foam. *Renewable Energy*, **149**, 208–216.
8. Abdelrahim, A. M., Abd El-Moghny, M. G., El-Sekhel, O. H., Salama, O. A., El-Shakre, M. E., & El-Deab, M. S. (2023). Wrapping massive MnO₂ around in-situ defective carbon felt with strong interaction for superb supercapacitive performance. *Colloids and Surfaces A: Physicochemical and Engineering Aspects*, **677**, 132441.
9. Nguyen, T. B., Yoon, B., Nguyen, T. D., Oh, E., Ma, Y., Wang, M., & Suhr, J. (2023). A facile salt-templating synthesis route of bamboo-derived hierarchical porous carbon for supercapacitor applications. *Carbon*, **206**, 383–391.
10. Trinh, K. T. & Tsubota, T. (2023). Supercapacitors composed of Japanese cedar bark-based activated carbons with various activators. *Materials Chemistry and Physics*, **307**, 128148.
11. Salama, R. S., Gouda, M. S., Aboud, M. F. A., Alshorifi, F. T., El-Hallag, A. A., &

- Badawi, A. K. (2024). Synthesis and characterization of magnesium ferrite-activated carbon composites derived from orange peels for enhanced supercapacitor performance. *Scientific Reports*, **14**(1), 8223.
12. Taer, E., Taslim, R., Mustika, W. S., & Fadli, E. (2021). Surface modification: unique ellipsoidal/strobili-fiber structure of porous carbon monolith for electrode supercapacitor. *Nanoscience and Technology: An International Journal*, **12**(4).
13. Nordenström, A., Boulanger, N., Iakunkov, A., Li, G., Mysyk, R., Bracciale, G., Bondavalli, P., & Talyzin, A. V. (2022). High-surface-area activated carbon from pine cones for semi-industrial spray deposition of supercapacitor electrodes. *Nanoscale Advances*, **4**(21), 4689–4700.
14. Damayanti, F., Astuti, I. P., Zulkarnaen, R. N., & Sunarti, S. (2020). Nutritional contents and the utilization of Indonesian native starfruits: *Averrhoa dolocarpa* and *A. leucopetala*. *Biodiversitas Journal of Biological Diversity*, **21**(4).
15. Anjarsari, S., Rahman, D. Y., & Sulistyowati, R. (2024). Pembuatan Bio-Baterai Berbahan Dasar Sari Belimbing Wuluh dan NaCl sebagai Sumber Ion serta Onggok Singkong sebagai Matriks. *Jurnal Penelitian Fisika dan Terapannya (JUPITER)*, **6**(1), 1–10.
16. Insan, R. R., Faridah, A., Yulastri, A., & Holinesti, R. (2019). Using belimbing wuluh (*averrhoa blimbi* l.) as a functional food processing product. *Jurnal Pendidikan Tata Boga Dan Teknologi*, **1**(1), 47–55.
17. Sharma, S. & Chand, P. (2024). Enhanced electrochemical performance of fabricated asymmetric supercapacitor in redox additive electrolyte. *Ceramics International*, **50**(3), 5775–5786.
18. Bandara, T. M. W. J., Alahakoon, A. M. B. S., Mellander, B. E., & Albinsson, I. (2024). Activated carbon synthesized from Jack wood biochar for high performing biomass derived composite double layer supercapacitors. *Carbon Trends*, **15**, 100359.
19. Diantoro, M., Aturroifah, N. I. M., Luthfiyah, I., Utomo, J., Hamidah, I., Yulianto, B., Rusydi, A., Maensiri, S., & Meevasana, W. (2025). 3D-porous activated carbon morphological modification of Manihot esculenta tuber and Bambusa blumeana stem for high-power density supercapacitor: Biomass waste to sustainable energy. *Carbon Resources Conversion*, 100313.
20. Lesbayev, B., Auyelkhankyzy, M., Ustayeva, G., Yeleuov, M., Rakhymzhan, N., Maltay, A., & Maral, Y. (2023). Recent advances: Biomass-derived porous carbon materials. *South African Journal of Chemical Engineering*, **43**(1), 327–336.
21. Qin, Q., Wang, J., Tang, Z., Jiang, Y., & Wang, L. (2024). Mesoporous activated carbon for supercapacitors derived from coconut fiber by combining H₃PO₄-assisted hydrothermal pretreatment with KOH activation. *Industrial Crops and Products*, **208**, 117878.
22. Agrawal, A., Gaur, A., & Kumar, A. (2023). Fabrication of *Phyllanthus emblica* leaves derived high-performance activated carbon-based symmetric supercapacitor with excellent cyclic stability. *Journal of Energy Storage*, **66**, 107395.
23. Kremer, L. S., Danner, T., Hein, S., Hoffmann, A., Prifling, B., Schmidt, V., Latz, A., & Wohlfahrt-Mehrens, M. (2020). Influence of the electrolyte salt concentration on the rate capability of ultra-thick NCM 622 electrodes. *Batteries & Supercaps*, **3**(11), 1172–1182.

24. Beyers, I., Bensmann, A., & Hanke-Rauschenbach, R. (2023). Ragone plots revisited: A review of methodology and application across energy storage technologies. *Journal of Energy Storage*, **73**, 109097.



This article uses a license
[Creative Commons Attribution
4.0 International License](https://creativecommons.org/licenses/by-nc/4.0/)